DO DAILY ACTIVITIES AFFECT GAS TAMPONADE–RETINA CONTACT AFTER PARS PLANA VITRECTOMY?

A Computational Fluid Dynamics Study

TOMMASO ROSSI, MD,* MARIA GRAZIA BADAS, PHD,† FEDERICO ANGIUS, DENG,† GIORGIO QUERZOLI, PHD†

Purpose: To calculate the retinal surface alternatively in contact with gas and aqueous because of fluid sloshing during daily activities such as ocular saccade, turning the head, standing up, and being a passenger of a braking car.

Methods: Fluid dynamics of aqueous and gas tamponade was reproduced using computational methods using the OpenFOAM open-source library. The double-fluid dynamics was simulated by the volume of fluid method and setting the contact angle at the aqueous–gas–retina interface.

Results: Sloshing increased the retinal surface in contact with aqueous by 13% to 16% regardless of fill rate and standing up determined the largest area of wet retina, followed by car braking, head rotation, and ocular saccade ($P < 0.001$). All activities except the ocular saccade determined a significant increase in the surface of retina in contact with the aqueous ($P < 0.005$). Car braking induced the highest shear stress (6.06 Pa); standing up determined the highest specific impulse and saccade the lowest.

Conclusion: Daily activities instantaneously reduce the amount of retina consistently in contact with gas tamponade and increase shear stress giving aqueous a potential access to the subretinal space regardless of patients' compliance.

RETINA 43:955–963, 2023

Pars plana vitrectomy is the preferred surgical technique for many types of retinal detachment, especially in pseudophakic eyes and in the presence of giant, multiple, or posterior retinal tears[1] and macular holes.[2]

Gas tamponade of varying duration is often injected after pars plana vitrectomy[3] to prevent aqueous from accessing retinal tears[4] until retinopexy establishes a solid retinal adhesion because fluid leakage into the subretinal space may lead to recurrent retinal detachment.

Patients are instructed to position after surgery so that the retinal tear(s) contact the shrinking gas bubble as long as possible.[5] In fact, gas tamponade reabsorption exposes increasing retinal portions to aqueous that may leak into the subretinal space through yet unsealed retinal tears.[6]

Although the gas–fluid interface and the fraction of retinal surface in contact with gas at rest have been thoroughly studied,[7,8] less is known about the extent of retinal surface affected by the sloshing of aqueous because of eye and patients' movements. During daily activities, retinal tears contacting gas under static conditions may temporarily fall under the air–fluid interface, giving aqueous a potential access to the subretinal space thus increasing the risk of recurrent retinal detachment or retinal shifting.

The purpose of this study was to calculate the extension of the retinal surface, temporarily wet by

From the *IRCCS Fondazione G.B. Bietti ONLUS, Roma, Italy; and †DICAAR, Università degli Studi di Cagliari, Cagliari, Italy.

None of the authors has any financial/conflicting interests to disclose.

Reprint requests: Tommaso Rossi, MD, IRCCS Fondazione Bietti ONLUS—Via Livenza 3, Roma 00198, Italy; e-mail: tommaso.rossi@usa.net

aqueous during daily activities, and as a function of gas fill.

Materials and Methods

Computational Fluid Dynamics Model

A numerical model was implemented within OpenFOAM[9] to simulate the flow of the gas and aqueous at rest and during the prescribed movements. It consists in resolving the mass conservation and Navier–Stokes equations together with an additional transport equation for the water volume fraction (volume of fluid technique[10]). The approach has already been successfully applied to the study of tamponades.[11,12]

The equations were solved over an unstructured mesh (consisting of 350,000 hexahedral and tetrahedral cells) generated by the "snappyHexMesh" tool, included in the OpenFOAM library. Five layers of hexahedral cells with progressively increasing height at the eye surface were extruded from the eye surface. The no-slip boundary condition was imposed at the walls for velocity, while a contact angle model was assumed to reproduce the gas–aqueous–retina interface behavior.

The pressure-implicit split-operator method[13] was adopted for solving the pressure–velocity coupling. Numerical integration was performed using second-order accurate schemes in space and first-order accurate, Euler scheme.

Physical properties of fluids used during the present simulations are summarized in Table 1.

Simulated Conditions

We investigated the statics of a patient standing in the upright position or supine and the dynamics of the following:

1. Sudden car braking;
2. Standing up from supine to sitting position;
3. Left–right head rotation; and
4. Saccadic motion.

Table 1. Physical Properties of Involved Fluids

	Air	Aqueous
Density	1 Kg/m^3	997 Kg/m^3
Dynamic viscosity	0.01813 mPa s	1 mPa s
Interfacial tension versus water	0.07 N/m	
Contact angle versus water and retina	16.2°	

In all the cases, 30%, 50%, and 80% volumetric tamponade filling fractions were considered.

The aim of the latter set of cases was to assess the impact of daily activities on the amount of retina remaining in contact with the tamponade and the shear stress caused by the fluid sloshing.

Car Braking

A 0.5 g (4.9 m/second^2) sudden car braking was simulated. The maneuver consists of three deceleration phases: a linear increase from zero to 0.5 g, a 1.0 seconds constant phase, and a linear decrease to zero in 0.1 seconds as the brake pedal is released. During the maneuver, the car speed drops from approximately 20 km/hour to zero. Deceleration and corresponding velocity–time laws are shown in Figure 1A. Although at the end of deceleration, the car is stationary, the computation is extended up to a total simulation time of 3 seconds to evaluate the tamponade behavior during its finale settling. At the end of the simulation, the tamponade interface reached the steady equilibrium again.

Standing up and head rotation. The time–laws of motion of standing up from supine to sitting position and the left–right head rotation were obtained recording the movement of a volunteer and tracking the eye's motion by means of image analysis techniques. The resulting time–laws (Figures 1, B–D) were implemented in the computational fluid dynamics model using the dynamic mesh technique. Figure 1B shows the eye trajectory during standing up from supine to sitting position (solid line) and lying down again (dashed line), while accelerations as functions of time are shown in Figure 1C. The whole movement lasts for 5 seconds. Figure 1D shows the eye rotation as a function of time in the case of head rotation (black line) and the corresponding angular acceleration (red line). The motion lasts for 2.2 seconds and achieves a maximum observed rotation angle as large as 66°.

Saccade. A horizontal saccade with 50° amplitude and 0.1375 seconds duration, attaining a 546.67°/s peak angular velocity, was simulated. It was obtained by the same polynomial law as in Rossi et al.[14] Figure 1E shows the eye rotation and the angular velocity as functions of time. The dynamic mesh technique was adopted to numerically simulate the prescribed motion.

Main outcome measures. The main study outcome measures include the retinal contact measured as the percentage value of retinal surface in contact with gas and aqueous, the shear stress at the retinal surface, and the specific impulse (SI). The vitreous chamber surface was divided into the following regions to better

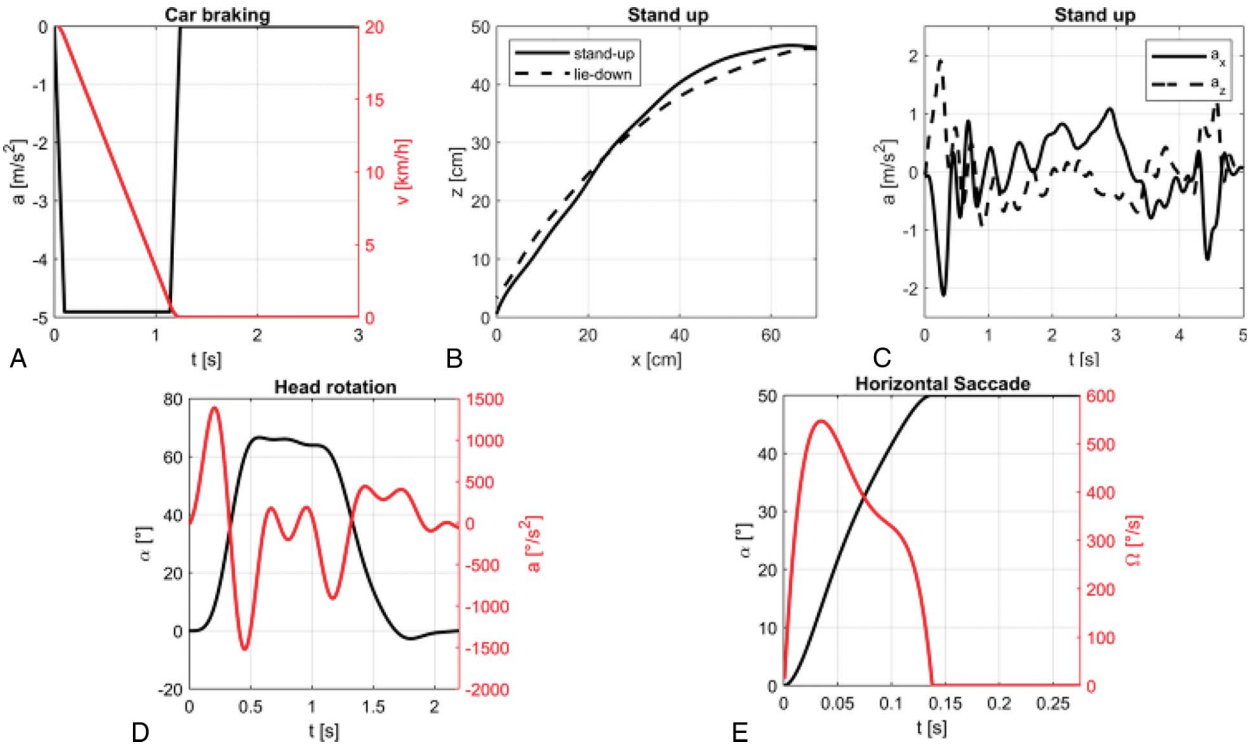

Fig. 1. Characterization of the simulated dynamical conditions: Car braking (**A**), standing up (**B** and **C**), head rotation (**D**), and saccade (**E**).

highlight the effect of the movement on the retina (Figure 2).

1. Macula (dark green): the retinal surface centered on the geometric posterior pole and extending 20° anteriorly;
2. Postequatorial retina (light green): the surface posterior to the geometric equator excluding the macula;
3. Preequatorial retina (blue): the surface anterior to the geometric equator comprised between the equator and the *pars plana*;
4. *Pars plana* ciliary body and posterior intraocular lens surface are represented in light blue and have been excluded from tamponade contact computation because they are retina. The presence of an artificial crystalline lens has been modeled because most eyes are rendered pseudophakic when gas tamponade is deemed necessary.

The SI describes the overall amount of solicitation on the retinal surface because of the considered activities. It is defined as the time integral of the instantaneous spatially averaged shear stress on the retinal surface:

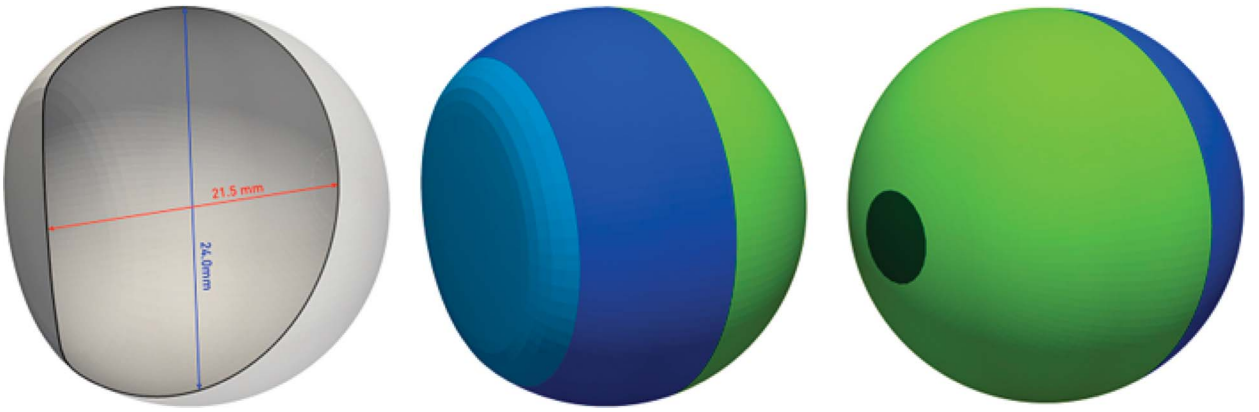

Fig. 2. Vitreous chamber morphology and segmentation. Light blue: pars plana; blue: preequatorial retina; green: postequatorial retina; and dark green: macula.

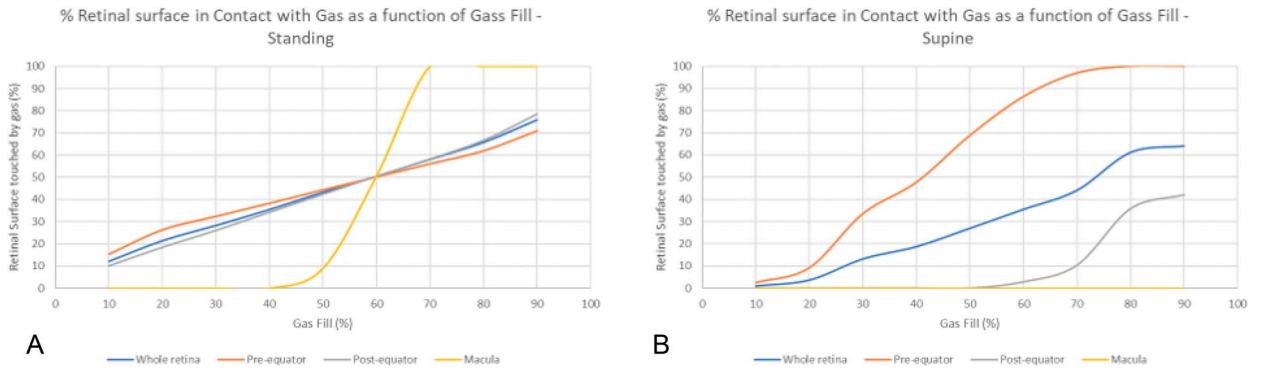

Fig. 3. Fraction of retinal surface in contact with gas under static conditions for a standing (**A**) and supine (**B**) patient as a function of the gas filling percentage.

$$\mathrm{SI} = \int_0^T \frac{1}{S} \int_S \mathrm{WSS}(t)\, dSdt$$

where WSS(t) is the instantaneous shear stress at each point of the retinal surface, T is the duration of the simulation, and S is the area of the retinal surface.

We introduced the SI because the considered motions differ significantly for both acceleration and duration. In addition, some of them include relatively long periods of time with low accelerations, e.g. during the two final seconds of the car braking or the second half of the simulation time in the saccade. These periods, although significant, would artificially decrease any time average.

Statistical analysis. The analysis of variance is applied to statistically evaluate the significance of shear stress values at different locations and to compare the outcomes obtained for different regions. The P values lower than 0.05 were considered statistically significant.

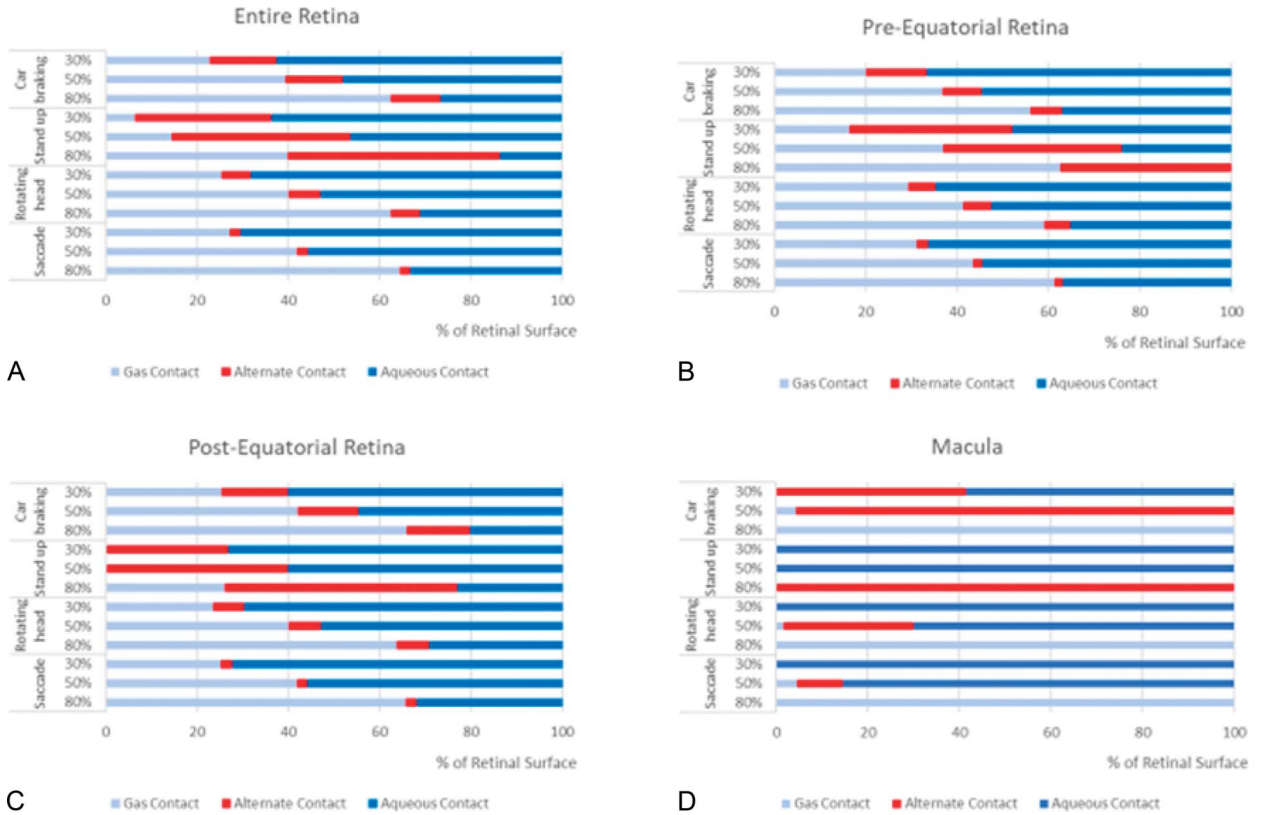

Fig. 4. Percentage of retinal surface in contact with gas (dry area, light blue bars), aqueous (wet area, dark blue bar) of wettable (red bar) for the considered daily activities and gas fill fractions.

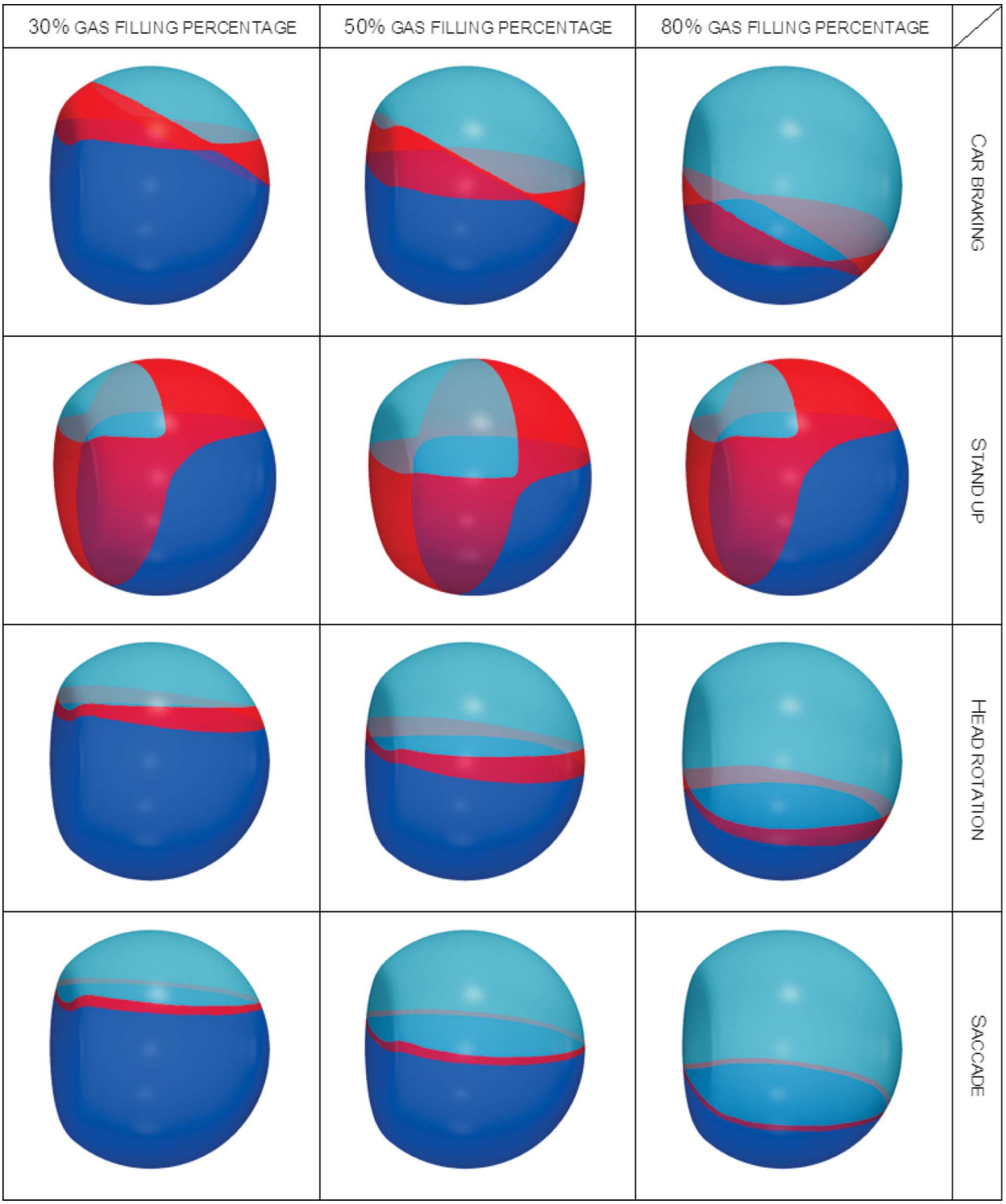

Fig. 5. Maps of wet, dry, and wettable areas for the four considered movements. Cyan areas are permanently in contact with the gas tamponade, blue areas are permanently wet by aqueous, and red areas come into contact both with tamponade and with aqueous during the motion.

Results

Gas–Retina Contact Under Static Conditions

The percentage of retinal surface touched by gas under static conditions for a supine and standing patient is shown in Figure 3.

Gas–Retina Contact Under Dynamic Conditions

Figure 4 shows the percentages of retinal surface wet by the aqueous during the whole motion time (blue bars), the surface percentages of retina always in contact with the tamponade (cyan bars), and the percentage wet by aqueous for a fraction of the motion and touching gas for the remaining time (red bars). Those will be hereafter referred to as "wet," "dry," and "wettable" areas, respectively (Figure 5).

Different activities significantly affected the retinal surface extension affected by fluid sloshing.

Standing up from the supine position determined the largest fraction of wettable retina, followed by car braking and ocular saccade (Figure 4; $P < 0.001$).

The extension of retina affected by aqueous sloshing was not significantly affected by gas fill irrespective of the considered activity (Figure 4 A–C) except for the macular region (Figure 4D), where the status of wet, dry, or wettable largely depended on gas fill ($P < 0.01$ for all activities except for the case of standing up).

When the wettable retinal surface is analyzed primarily as a function of gas fill (Figures 5 and 6), it becomes apparent that standing up exposes the largest retinal surface to aqueous contact (more than 60%) even at 80% gas fill and more than 90% at 30% filling percentage. At 50% gas fill, all other activities expose 50% to 60% of the postequatorial retina to aqueous (Figure 6C), while the preequatorial retina (where most retinal tears occur) is significantly less wettable only for the standing-up activity ($P < 0.05$). Regardless of gas fill percentage, all activities except the ocular saccade determined a significant increase in the surface of retina in contact with aqueous (wettable area; $P < 0.005$ except for the macula).

The mean percentage of "wettable" retina during all considered activities is summarized in Table 2 regardless of gas fill, between 13% and 16% of the entire retinal surface intermittently contacted aqueous. There was no significant difference across the different retinal sectors and/or gas fill.

Shear Stress

Car braking induced a significantly higher shear stress (6.06 Pa, $P = 0.018$) than any other activity regardless of the fill fraction (Figure 7; $P < 0.05$). The lower gas fill simulations returned significantly higher shear stress values for all considered activities

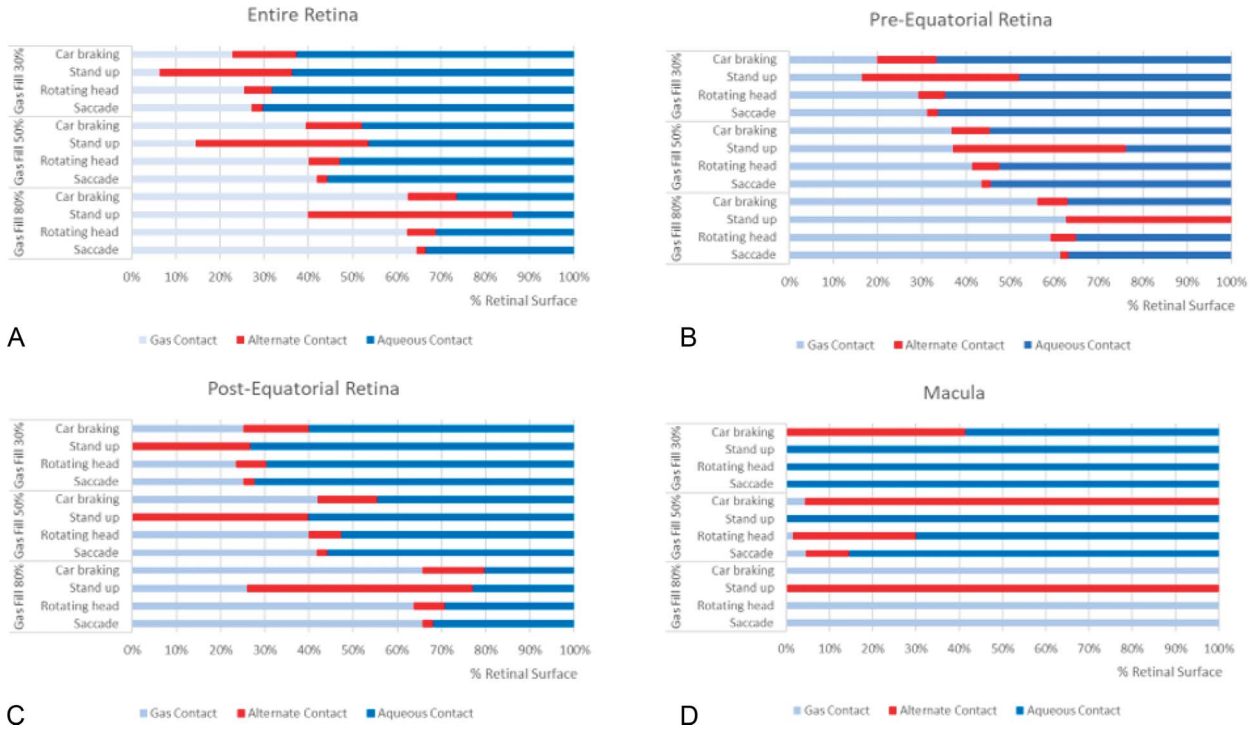

Fig. 6. Proportion of retinal surface in contact with gas (dry, light blue bar), aqueous (wet, dark blue bar) of wettable (red bar) for each considered activity and gas fill percentage.

Table 2. Average Percentage of Retinal Surface Becoming "Wet" During all Considered Activities

Gas Fill	Entire Retina	Preequator	Postequator	Macula	*P*
30%	13.3 ± 10.2	14.3 ± 12.2	12.7 ± 9.2	10.3 ± 17.9	n.s.
50%	15.2 ± 14.2	13.9 ± 14.7	15.7 ± 14.5	33.5 ± 37.3	n.s
80%	16.5 ± 17.5	13.0 ± 14.2	18.6 ± 19.2	25.0 ± 43.3	n.s
P	n.s.	n.s.	n.s.	n.s	

($P < 0.05$) except for standing up when the 50% gas fill reached the highest shear stress.

Specific Impulse

The specific impulse was significantly different among activities (Figure 8; $P < 0.001$); standing up determined a significantly higher SI and the saccade lower SI than any other activity. Gas fill did not significantly affect SI (Figure 8).

Discussion

Maintaining retinal tears in contact with gas as long as possible is important to promote long-term adhesion after retinal detachment surgery[15–17] and represents the rationale of patients positioning according to the tears location.[18] Patients' compliance has also been demonstrated to significantly influence anatomical outcome,[19] and devices intended to favor, alert, instruct, and keep record of adherence to those instructions have been proposed.[20,21] Vitrectomy without the use of any gas tamponade, conversely, has been advocated as an alternative by many authors and for different indications[22–24] because the need for positioning significantly disrupts the daily routine.

Irrespective of patients' willingness and ability to comply with prescribed positioning, the daily activities significantly affect the proportion of "dry" and "wet" retina as the dynamics of eye and head motion determines fluid sloshing and a third "gray" zone of "wettable" or alternatively "dry" and "wet" retina creates. Our data show that during such activities, an average 15% of the overall retinal surface (Table 2) temporarily loses its contact with gas regardless of gas fill and patients' compliance.

It is interesting to note that as gas fill reduces, the extension of "wettable" retina does not significantly change for any considered activity (Figures 4–6), thus acquiring more proportional importance. In other words, the "wettable" retinal surface to be added to "wet" retina remains fairly invariant, while gas bubble reduces its volume.

Not surprisingly, standing up causes the largest variation of wettable retinal surface as it implies the transition from supine to standing posture so that approximately half the retinal surface is affected by a change in gas/fluid contact, even with almost complete gas fill. Deceleration associated to car braking represented the second most important activity in retinal surface becoming "wet," followed by head rotation and eye saccade. This means that stenopeic goggles once advocated to keep the eye in primary position would very marginally help because head motion seems more important than eye motion, as also reported by Angunawela et al.[25]

The macula deserves a separate mention because it is the site for specific pathology (macular holes and myopic retinal detachment within the staphyloma only to name a few) and is extremely sensitive to both head positioning and gas fill. Figures 4–6 show how the macula becomes temporarily wet during virtually all activities unless when gas fill is very high. This notion suggests that a higher compliance with positioning is advisable after macular surgery especially in highly myopic eyes[19] as well as the use of longer-lasting gases.

Across considered activities and gas fill fraction, the preequatorial retina (Figure 6) maintained a much larger gas contact, on average, than the postequatorial, which became almost entirely "wet." Because many challenging retinal tears occur posterior to the equator,[26] the patient should be instructed to reduce head motion as much as possible and longer-acting gases are preferred under those circumstances also.

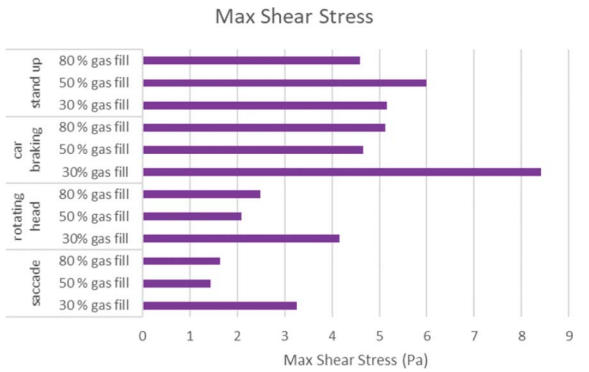

Fig. 7. Maximum shear stress for each inquired retinal section and patient activity standing up (**B** and **C**), head rotation (**D**), and saccade (**E**).

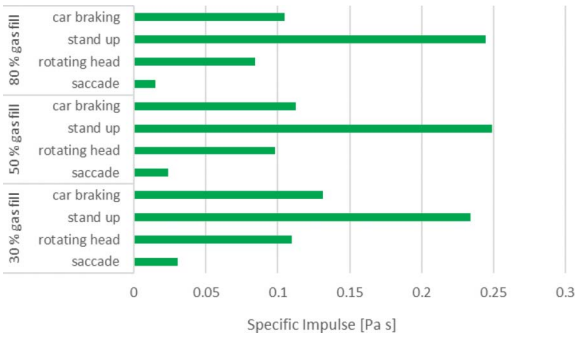

Fig. 8. Specific impulse for each activity and as a function of gas fill percentage. Note how activity determines the magnitude of SI, whereas gas fill does not significantly affect it.

Whether the shear stress generated by aqueous sloshing can elevate retinal tears and allow fluid into the subretinal space is a lengthy debated issue.[18] Retinal adhesion strength has been estimated across a broad range (4–266 Pa),[27–29] and it is known to temporarily decline after retinopexy[30] to less than 4 Pa or approximately 50% of the initial strength after 8 hours and then increase within 24 hours[31]; such values are lower than those calculated in our model and suggest this mechanism is conceivable. Although it is simplistic to believe that this is the only or main factor responsible for retinal redetachment, many activities resulted in shear stress exceeding this value (Figure 7).

Magnitude combined to the duration of applied shear stress may also concur in defining the activities to be restricted: Standing up determined the largest SI regardless of gas fill percentage (Figure 8), followed by car braking and turning head. The ocular saccade being almost instantaneous seemed safer than all other activities for this standpoint.

In summary, our study shows that along with portions of the retina known to be consistently in contact with gas or aqueous as a function of gas fill at rest, patients' activities cause a significant proportion of retinal surface to become momentarily wet by aqueous regardless of patients' compliance. This should be considered by surgeons because sloshing significantly reduces the amount of retina to be considered permanently "dry" and therefore "safe." Surgeons should also be aware that the shear stress and SI determined by the sloshing may exceed the retinal adhesion force, concurring to aqueous leaking into the subretinal space and possibly retinal shifting, therefore instructing patients to longer or different positioning and/or using longer-acting cases if deemed necessary.

Key words: pars plana vitrectomy, computational model, computational fluid dynamics, gas tamponade, shear stress.

Acknowledgments

The authors thank the "Fondazione Roma," the Italian Ministry of Health and CINECA (within study IsC99 "Fluos"), for financial support.

References

1. Amara A, Bernabei F, Chawki MB, et al. Comparison between air and gas as tamponade in 25-gauge pars plana vitrectomy for primary superior rhegmatogenous retinal detachment. Eye (Lond) 2021;36:2028–2033.
2. Romano MR, Rossi T, Borgia A, et al. Management of refractory and recurrent macular holes: a comprehensive review. Surv Ophthalmol 2022;67:90800007–90809318.
3. Neffendorf JE, Gupta B, Williamson TH. The role of intraocular gas tamponade in rhegmatogenous retinal detachment: a synthesis of the literature. Retina 2018;38:S65–S72.
4. Gozawa M, Kanamoto M, Ishida S, et al. Evaluation of intraocular gas using magnetic resonance imaging after pars plana vitrectomy with gas tamponade for rhegmatogenous retinal detachment.Sci Rep. 2020;10:1521.
5. Hostovsky A, Mandelcorn MS, Mandelcorn ED. Orbital magnetic resonance imaging demonstrates better contact between the gas and anterior inferior retina in side versus face-down position. Ophthalmol Retina 2020;4:911–918.
6. Govers BM, Lamers MPM, Klevering BJ, Keijser S. Air versus fluorinated gas tamponades in pars plana vitrectomy treatment for primary rhegmatogenous retinal detachment. Acta Ophthalmologica 2022;100:e1600–e1605.
7. Eames I, Angunawela RI, Aylward GW, Azarbadegan A. A theoretical model for predicting interfacial relationships of retinal tamponades. Invest Ophthalmol Vis Sci 2010;51:2243–2247
8. Hartmann GC. Physical model for absorption of intraocular gas. Digit J Ophthalmol 2013;19:18–20
9. Greenshields C, Weller H. Notes on Computational Fluid Dynamics: General Principles. 2022. ISBN 978-1-3999-2078-0. Reading, UK: CFD Direct Ltd.
10. Hirt CW, Nichols BD. Volume of fluid (VOF) method for the dynamics of free boundaries. J Comput Phys 1981;39:201–225.
11. Rossi T, Querzoli G, Badas MG, et al. Computational fluid dynamics of intraocular silicone oil tamponade. Translational Vis Sci Technol 2021;10:22.
12. Rossi T, Querzoli G, Badas MG, et al. Silicone oil tamponade–retina contact in highly myopic eyes with and without encircling bands: a computational fluid dynamics study. Translational Vis Sci Technol 2022;11:1.
13. Ferziger JH, Perić M. Solution of the Navier-Stokes equations. In: Ferziger JH, Perić M, eds. Computational Methods for Fluid Dynamics. New York, NY, USA: Springer; 2002:157–216. doi. 10.1007/978-3-642-56026-2_7
14. Rossi T, Badas MG, Querzoli G, et al. Does the Bursa Pre-Macularis protect the fovea from shear stress? A possible mechanical role. Exp Eye Res 2018;175:159–165.
15. Parver LM, Lincoff H. Geometry of intraocular gas used in retinal surgery. Mod Probl Ophthalmol 1977;18:338–343.
16. Casswell EJ, Yorston D, Lee E, et al. Effect of face-down positioning vs support-the-break positioning after macula-involving retinal detachment repair: the PostRD randomized clinical trial. JAMA Ophthalmol. 2020;138:634–642.

17. Otsuka K, Imai H, Miki A, Nakamura M. Impact of postoperative positioning on the outcome of pars plana vitrectomy with gas tamponade for primary rhegmatogenous retinal detachment: comparison between supine and prone positioning. Acta Ophthalmol 2018;96:e189–e194.
18. Chen X, Yan Y, Hong L, Zhu L. A comparison of strict facedown positioning with adjustable positioning after pars plana vitrectomy and gas tamponade for rhegmatogenous retinal detachment. Retina 2015;35:892–898
19. Pasu S, Bell L, Zenasni Z, et al. Positioning in macular hole surgery (pims) study group. Facedown positioning following surgery for large full-thickness macular hole: a multicenter randomized clinical trial. JAMA Ophthalmol. 2020;138:725–730.
20. Brodie FL, Ramirez DA, Pandian S, et al. Novel positioning sensor with real-time feedback for improved postoperative positioning: pilot study in control subjects. Clin Ophthalmol 2017;11:939–944.
21. Brodie FL, Woo KY, Balakrishna A, et al. Validation of sensor for postoperative positioning with intraocular gas. Clin Ophthalmol 2016;10:955–960
22. Martínez-Castillo V, Zapata MA, Boixadera A, et al. Pars plana vitrectomy, laser retinopexy, and aqueous tamponade for pseudophakic rhegmatogenous retinal detachment. Ophthalmology 2007;114:297–302.e1.
23. Sato T, Emi K, Bando H, Ikeda T. Retrospective comparisons of vitrectomy with and without air tamponade to repair lamellar macular hole. Ophthalmic Surg Lasers Imaging Retina 2015;46:38–43.
24. Lee KH, Chung YR, Yeo S, et al. Is gas/air tamponade essential for eyes with small peripheral retinal breaks without detachment during vitrectomy? BMC Ophthalmol. 2022;22:186.
25. Angunawela RI, Azarbadegan A, Aylward GW, Eames I. Intraocular fluid dynamics and retinal shear stress after vitrectomy and gas tamponade. Invest Ophthalmol Vis Sci 2011;52:7046–7051.
26. Abdolrahimzadeh S, Piraino DC, Scavella V, et al. Spectral domain optical coherence tomography and B-scan ultrasonography in the evaluation of retinal tears in acute, incomplete posterior vitreous detachment. BMC Ophthalmol 2016;16:60.
27. DeGuillebon H, Zauberman H. Experimental retinal detachment. Biophysical aspects of retinal peeling and stretching. Arch Ophthalmol 1972;87:545–548.
28. Kita M, Marmor MF. Retinal adhesive force in living rabbit, cat, and monkey eyes. Normative data and enhancement by mannitol and acetazolamide. Invest Ophthalmol Vis Sci 1992;33:1879–1882.
29. Kain HL. A new model for examining chorioretinal adhesion experimentally. Arch Ophthalmol 1984;102:608–611.
30. Kain HL. Chorioretinal adhesion after argon laser photocoagulation. Arch Ophthalmol 1984;102:612–615.
31. Yoon YH, Marmor MF. Rapid enhancement of retinal adhesion by laser photocoagulation. Ophthalmology 1988;95:1385–1388.